上海交通大學

SHANGHAI JIAO TONG UNIVERSITY

学士学位论文

THESIS OF BACHELOR

论文题目：胆甾液晶的积分方程和密度泛函理论研究

学生姓名：文　聪

学生学号：516111910163

专　　业：化学（致远荣誉计划）

指导教师：吴量

学院(系)：化学化工学院，致远学院

上海交通大学
学位论文原创性声明

本人郑重声明：所呈交的学位论文，是本人在导师的指导下，独立进行研究工作所取得的成果。除文中已经注明引用的内容外，本论文不包含任何其他个人或集体已经发表或撰写过的作品成果。对本文的研究做出重要贡献的个人和集体，均已在文中以明确方式标明。本人完全意识到本声明的法律结果由本人承担。

学位论文作者签名：某某

日　期：某年某月某日

上海交通大学
毕业设计（论文）版权使用授权书

本毕业设计（论文）作者完全了解学校有关保留、使用毕业设计（论文）的规定，同意学校保留并向国家有关部门或机构送交论文的复印件和电子版，允许论文被查阅和借阅。本人授权上海交通大学可以将本毕业设计（论文）的全部或部分内容编入有关数据库进行检索，可以采用影印、缩印或扫描等复制手段保存和汇编本毕业设计（论文）。

保　密 □，在 _____ 年解密后适用本授权书。

本学位论文属于

不保密 □。

（请在以上方框内打“✓”）

学位论文作者签名：　　指导教师签名：

日期：　　年　　月　　日　　日期：　　年　　月　　日

胆甾液晶的积分方程和密度泛函理论研究

摘　要

对于一类特殊的分子，在计算机分子模拟中观察到了其胆甾相（手性向列向），但整个计算过程仍然非常耗时，所以我们构建了一个可以更加便捷地预测这类分子热力学性质的理论框架。理论体系以 Onsager 的液晶相变理论为基础，以 Parsons-Lee 的硬球近似方法为改进，我们可以用密度泛函理论（DFT）计算出这类分子的径向分布函数（ODF）。为了预测其胆甾相，我们进一步使用 Straley 的近似方法，以向列相的 ODF 近似为胆甾相的局部 ODF，从而可以预测得到液晶分子在胆甾相下的热力学性质。

关键词：液晶，统计力学，密度泛函理论

THE INTEGRAL EQUATION AND DENSITY FUNCTION THEORY OF CHOLESTERIC LIQUIDS

ABSTRACT

Cholesteric phase is found for certain liquid crystals molecules in computer simulation, but the process is still very time-consuming, so we constructed a theoretical framework to predict the thermodynamic properties of this molecule. Based on Onsager's theory and Parsons-Lee's improvement of phase transition of liquid crystals, we used density function theory to calculate the orientational distribution function of the molecule. And in addition, by applying Straley's approximation method, we calculated the cholesteric pitches for a given density. We thus found a way to predict the thermodynamic properties of cholesteric liquid crystals.

Key words: Liquid Crystal, Statistical Mechanics, Density Function Theory

Contents

List of Figures

List of Tables

List of Algorithms

Nomenclature

ϵ_0	Energy Unit
k	Boltzmann Constant
T	Temperature
β	$\frac{1}{kT}$
O	Ensemble Average of a Physical Property
O^*	Reduced Ensemble Average of a Physical Property
F	Free Energy
P	Pressure
μ	Chemical Potential
p	Cholesteric Pitch
q	$2\pi/p$, Cholesteric Pitch Wave Vector
$f(\vec{u})$	Orientational Distribution Function(ODF)
v_m	Molecular Volume
ρ	Number Density
η	ρv_m, Packing Fraction

Chapter 1 Introduction

1.1 Liquid Crystals

Liquid crystals are a special material which behaves between conventional liquids and solid crystals. They might flow like a liquid, but they preferred to be oriented in a crystal-like way. Historically, liquid crystals were discovered in 1888 when the Australian botanist Friedrich Reinitzer studied cholesterol benzoate, which is now known as cholesteric liquid crystals, and his friend German physicist Otto Lehmann named it "Liquid Crystal".

Overall liquid crystals can be classified into thermodynamic ones and lyotropic ones. The classification is according to the required condition of phase transition, thermodynamic liquid crystals undergo a phase transition as temperature is changed while the lyotropic liquid crystals undergo a phase transition as concentration is changed. In theoretical study we always use packing fraction instead of concentration. In natural environment they mainly consist of organic molecules and few minerals and in technological application they are more common, which can be used in electronic components or in liquid crystal displayers. They are also common in biology, for example tobacco mosaic virus, in which the ratio of length and thickness is around 15.

Microscopically, liquid crystals are mostly rod-like or plate-like molecules, which enables them to behave anisotropically under certain circumstances. There are several typical phases which can arise under certain circumstances for a given molecule, and the schematic figure is given below.

Isotropic Phase Isotropic phases are the most common phases in any conventional liquid, this will happen if the temperature is too high (so that the kinetic energy dominates) or the density is too low (so that every molecule has much more space to move around). In any cases molecules can move freely regardless of its rod-like (or plate-like) shape, and they behaves just like conventional fluids.

Nematic Phase This is one of the most common anisotropic phase in liquid crystals. The term originates from Greek and means thread-like. Although the position of center of mass of them are still randomly distributed, they form a long-range directional order with their long axes nearly parallel. This always happens in relatively high density or low temperature condition (so that the interaction between molecules will dominate over kinetic energy). In this case molecules are pushing each other and tend to lean on each other in a nearly parallel way. The director (preferred direction) $n(r)$ is assumed to be invariant in the whole space in theoretical work.

Smectic Phase Smetic phase is observed in a much lower temperature than that of nematic phase, molecules are more ordered in this phase than that in nematic phase, they have a preferred direction as in nematic phase, and in addition the position of center of mass is ordered along one direction.

Cholesteric Phase It is more often called the chiral nematic phase, the name comes from the choleterol derivatives from which this phase was first observed. Only chiral molecules can give rise to such a phase. The chiral interaction between molecules will result in asymmetric packing,

and further results in long-range chiral order. The twisting of molecules is perpendicular to local director. So there is a azimuthal twist between two layers, and on each layer the molecules behave like nematic phase, this is why is called the "chiral nematic phase". To be more precise theoretically, the director $n(r)$ in cholesteric phase is not invariant in the whole space, it is rotating along a direction perpendicular to itself. The distance between two layers over which the molecules undergo a 360° twist, is the chiral pitch. The larger the chirality in molecule is, the smaller the pitch is.

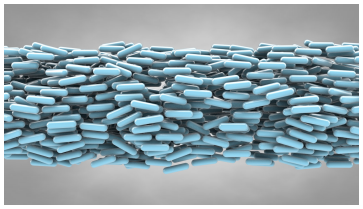

Figure 1–1 Nematic Phase

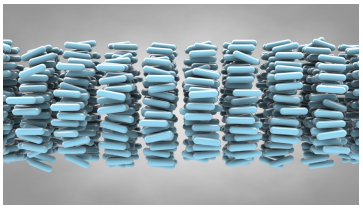

Figure 1–2 Smectic Phase

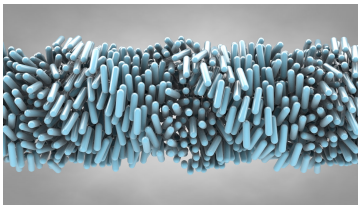

Figure 1–3 Cholesteric Phase

There are also other phases such as blue phase (which take place between cholesteric phase and isotropic phase), discotic phases and conic phases are also observed in various molecules, and we omit the detailed explanation here.

1.2 Related Theoretical Work

The theory of liquid crystal originates from Lars Onsager's seminar work[1] in 1949, to investigate how the phase transition happens and provide insight into the relationship between microscopic molecular characteristics and the macroscopic phase behavior, he considered the cylinders with large aspect ratio (the quotient of length and diameter $\kappa = L/D$), due to the spontaneous symmetry breaking in these kind of molecules, the distribution of orientation was not uniform, this is where the DFT theory come into play. He calculated the theoretical transition point of isotropic-nematic phase using Onsager's trial function. Oblate ($\kappa < 1$) and prolate ($\kappa > 1$) ellipsoids are also well-studied. In addition, the theories on soft[2] and hard spherocylinders[3] are also developed.

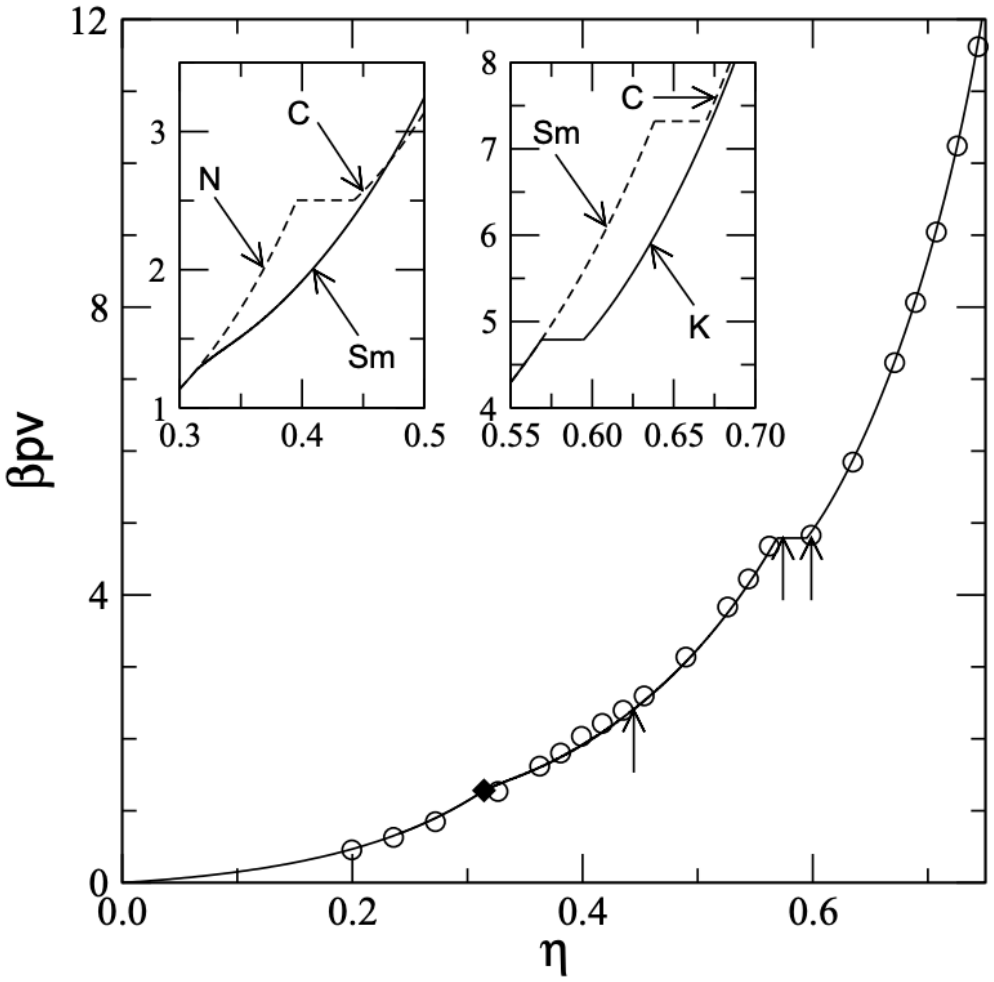

Figure 1–4 Phase diagram of Hard Cylinders[4]

At the beginning of 20th century, Born attributes the behavior of liquid crystals to the long-range electric interaction. Based on this viewpoint Maier and Saupe developed a phase transition theory, taking the dispersion forces between molecules and described the phase transition from isotropic to nematic. The Maier-Saupe theory provided a method which can effectively describe the temperature dependency and was used widely in thermodynamic liquid crystals. But the shape of the molecules which can significantly influence the anisotropicity of the molecule, was not taken care in the theory, so it was not suitable to describe lyotropic liquid crystals. Kimura combined Onsager's original model and dispersion forces, and described the isotropic-nematic phase transition by introducing the field of mean potential and a temperature-dependent order parameter. Further the dipole interactions are introduced, McGother used Monte Carlo method in canonical ensemble and simulated hard cylinders with dipole interactions, it turns out that in the case smetic phase was more likely to form than nematic phase. The series of studies showed that the phase behavior is in tight correlation with the long-range interactions (dispension forces, dipole interactions...)

This are also a number of ordinary cholesteric liquid crystals, the underlying reasons of their

formation is still challenging. There are many research results showing that the long-range interaction is an important factor in the formation of cholesteric liquid crystals, for example, filamentous viruses[5], actins[6], cellulose derivatives[7], single-walled carbon nanotubes[8]. There are also a lot of work on proposing a practical chiral-interaction between hard particles to reproduce the cholesteric phase, such as the Gossens model[9], patchyrod model[10] (our FCh is one of these).

1.3 Arrangement of The Thesis

This undergraduate thesis mainly investigated electrically neutral lyotropic liquid crystals, this is a kind of typical soft matter. The understanding of liquid crystal at a molecular level is still challenging, in a preceding work by Liang[11], a coarse-grained molecular model is developed and represented by flexible chain with helical interactions (FCh). Since the molecular dynamics simulation is still limited by many factors, such as the different interactions involved, and the concrete simulation conditions. So developing general framework for predicting such liquid crystals is significant, as we will see in the following chapters, this general theoretical method can be applied to various kinds of liquid crystals and only take fewer time to predict the thermodynamic properties of certain molecules.

A theoretical method is developed in this thesis to give a prediction of thermodynamic properties of FCh model. The theory was based on Onsager's original theory of phase transition of liquid crystals, and made use of DFT method to give a depiction of the thermodynamic properties of the phase transition of FCh. In addition, a modular program is developed from scratch for the phase diagram computation of a wide range of liquid crystal molecules including FCh.

The thesis will first show introduce the DFT method in general case in Chap. 2, describing our theoretical method, we construct a theoretical framework to illustrate how the computation goes , in particular, we stated basic results in Onsager's original theory, which incorporates the ODF for the first time, and then introduce the Parsons-Lee's approximation, the method improves the original theory by a multiplicative coefficient, then Straley's approximation method is introduced when trying to find the cholesteric phase. Then we are going to study in Chap. 3 our molecular model and the existing simulation result, we further derive the thermodynamic properties of FCh by applying DFT method, and illustrating concrete Monte Carlo method involved in order to compute complicated integrals. We showed typical results and compared with simulation on the transition point isotropic-nematic phases.

Chapter 2 Density Function Theory

In this section we will introduce the density function theory (DFT) from scratch and particularly focus on how to use it in the prediction of liquid crystals, and then introduce the Parsons-Lee's approximation and Straley's method which can significantly improve the original theory of Onsager. Finally we introduce a general iteration method to solve DFT.

Before formally introducing density function theory, we have to recapitulate some of the basic conclusions in ensemble theory.

2.1 Ensemble Theory

Tab. 2–1 is a summary of three most common ensembles, and we give below the formulas to derive other physical properties in case of canonical system and grand-canonical system, these are important in the following derivations.

Table 2–1 Summary of Ensembles

System	Condition	Ensemble	Partition Function	Probability $p(s)$
Isolated system	E, N, V fixed	micro-canonical	$\Omega(E, V, N)$	$\frac{1}{\Omega(E, V, N)}$
Closed system	N, V fixed	canonical	$Z(T, V, N)$	$\frac{e^{-\beta E_s}}{Z(T, V, N)}$
Open system	V fixed	grand-canonical	$\Xi(T, V, \mu)$	$\frac{e^{-\beta(E_s-\mu N_s)}}{\Xi(T, V, \mu)}$

The relations between partition function

$$Z(T, V, N) = \sum_s e^{-\beta E_s} = \sum_E \Omega(E, V, N) e^{-\beta E},$$
$$\Xi(T, V, \mu) = \sum_s e^{-\beta(E_s-\mu N_s)} = \sum_N Z(T, V, N) e^{\beta N \mu}.$$

2.1.1 Minimal Free Energy Principle

In fact, in equilibrium statistical mechanics, we have several equivalent principles (postulates), we list them here without reasoning, because the readers should be familiar with all of this at their first course of thermodynamics.

Postulate of Equal *a prior* probability For an isolated system with given (E, V, N), the system can be found with equal probability in any microstate.

principle of Maximal Entropy For an isolated system, the Gibbs entropy reaches its maximal at its equilibrium state.

principle of Minimal Free Energy For a closed system, the Helmholtz free energy reaches its minimal at its equilibrium state.

principle of Maximum Work For a closed system, the maximal work which the system is capable to do to the environment in a given process is the change in Helmholtz free energy.

2.1.2 Ideal Gases

This part will contain the concrete calculation of partition function of a system, in particular, ideal gas.

In a classical system, the space is continuous, hence the summation $\sum_s$ becomes the integration in phase space $\int \prod \mathrm{d}\, p_i \,\mathrm{d}\, q_i$, in which p and q are all 3-dimensional vector, and i is taken over all N particles. The canonical partition function then reads

$$Z(T,V,N) = \frac{1}{h^{3N}N!}\int \prod_i \mathrm{d}\, p_i \,\mathrm{d}\, q_i e^{-\beta H(p,q)}, \tag{2–1}$$

in which coefficient h^{3N} is proposed by Landau to nondimensionalize the partition function, and coefficient $N!$ is proposed by Gibbs to tackle the distinguishability of identical particles.

As for ideal gas, the Hamiltonian writes

$$H_{id} = \sum_i \frac{p_i^2}{2m}, \tag{2–2}$$

hence the integral in the partition function Z can be computed directly,

$$Z(T,V,N) = \frac{V^N}{h^{3N}N!}\left(\int \mathrm{d}\, p e^{-\beta p^2/2m}\right)^N = \frac{V^N}{N!\Lambda^{3N}}, \Lambda = \frac{h}{\sqrt{2\pi mkT}}, \tag{2–3}$$

in which the second equality is got from Gaussian integral, then the free energy can be computed

$$\frac{F_{id}}{N} = -\frac{kT}{N}\ln Z(T,V,N) = kT\left[\ln(\rho\Lambda^3) - 1\right], \tag{2–4}$$

in which $\rho = N/V$ is the number density.

As for the calculation of ideal gases, we stop here for convenience, because it is easy to further compute pressure, chemical potential, entropy from its derivative. We proceed to do this when tackling the liquid crystal model.

2.1.3 Non-ideal Gases

As for non-ideal gases, there is mutual interaction between molecules, as in most common cases, only two-body interaction is involved, so the Hamiltonian can be written as

$$H_{ni} = \sum_i \frac{p_i^2}{2m} + \sum_{i<j} u(q_i, q_j). \tag{2–5}$$

Now the partition function can be again computed

$$Z(T,V,N) = \frac{Q_N}{N!\Lambda^{3N}}, \tag{2–6}$$

in which the denominator comes from kinetic energy while the enumerator Q_N is the configurational integral, and comes from potential energy,

$$Q_N = \int \prod_i \mathrm{d}\, q_i \prod_{i<j} e^{-\beta u(q_i, q_j)}. \tag{2–7}$$

So in this case the free energy is given by

$$F_{ni} = -kT \ln Z(T, V, N) = -kT \ln \frac{V^N}{N! \Lambda^{3N}} - kT \ln \frac{Q_N}{V^N} = F_{id} - kT \ln \frac{Q_N}{V^N}. \tag{2–8}$$

Mayer's is function is defined as $f_{ij} = e^{-\beta u(q_i, q_j)} - 1$ and used to tackle the integration in Q_N,

$$\begin{aligned} Q_N &= \int \prod_i \mathrm{d}\, q_i \prod_{i<j} (f_{ij} + 1) \\ &= V^N \left[1 + \frac{N^2}{V} \int f(q)\, \mathrm{d}\, q + \mathcal{O}(f^2) \right]. \end{aligned} \tag{2–9}$$

Then the expression of F can be written as

$$F_{ni} = F_{id} + kT \frac{N^2}{V} B_2 + \cdots, \tag{2–10}$$

in which B_2 is the second Virial coefficient, it is also a half of the excluded volume

$$B_2 = -\frac{1}{2} \int f(q)\, \mathrm{d}\, q. \tag{2–11}$$

Now we give how physical properties can be computed from the partition function.

In the canonical ensemble, we have

$$\begin{aligned} F(T, V, N) = -\frac{1}{\beta} \ln Z(T, V, N) = E - TS, \\ S = -\frac{\partial F}{\partial T}, P = -\frac{\partial F}{\partial V}, \mu = \frac{\partial F}{\partial N}. \end{aligned} \tag{2–12}$$

In the grand-canonical ensemble, we have

$$\begin{aligned} \Phi(T, V, \mu) = -\frac{1}{\beta} \ln \Xi(T, V, \mu) = -PV, \\ S = -\frac{\partial \Phi}{\partial T}, P = -\frac{\partial \Phi}{\partial V}, N = -\frac{\partial \Phi}{\partial \mu}. \end{aligned} \tag{2–13}$$

2.2 Density Function Theory

The most important physical principle in density function theory is the minimal free energy principles, which has been stated in the previous section. The equilibrium single-particle density of a system is a function of its position, to be more precise, it is a function in the whole configuration space with integral 1, as for spherically symmetric particles, the density is given by $\rho(q)$, in which q is the generalized coordinates for position. As for a rotational symmetric uniaxial molecule, the density function is given by $\rho(q, u)$, in which u is the generalized coordinate for orientation, in practice it is a vector on a unit sphere.

In the latter case for a uniaxial molecule, the density function can be expresser in terms of Dirac's delta function:

$$\rho(q, u) = \left\langle \sum_{i=1}^{N} \delta(q_i - q) \delta(u_i - u) \right\rangle \tag{2–14}$$

The bracket means an ensemble average. In homogeneous case, we know $\rho(q,u)$ is a constant, in a nematic phase, the molecules will be preferentially ordered along a director, but the distribution of position is still uniform, this gives that

$$\rho_{ne}(q,u) = \rho\varphi(u), \tag{2–15}$$

in which ρ is the mean number density, and $\varphi(u)$ is the so-called orientational distribution function (ODF), and it is normalized to 1. As for smetic-A phases, the molecules are not only orientationally ordered, but also translationally ordered along the preferred director. Now the density function is given by

$$\rho_{sA}(q,u) = \rho_{sA}(q_z,u), \tag{2–16}$$

if l is defined as the smetic layer thickness, then ρ is a periodic function in z, with periodicity l.

Density function theory allows us to find out the single-particle density without the definition Eqn. 2–14, instead, the principle of minimal free energy is used, and the density function which made free energy minimal is the desired result of real density function.

2.3 Liquid Crystal Theory of Onsager

This theory is based on the famous paper[1] of Onsager in 1949. Instead of spheres, we consider cylinders as our model of a molecule. It is discovered that liquid crystals undergoes an isotropic-nematic phase transition at low temperature and high density. Due to the spontaneous rotational symmetry breaking, the postulate of equal *a prior* probability no more makes sense, so Onsager proposed to assume that there exists a particular director as the previous analysis shows. And assume $\rho_{ne}(q,u) = \rho\varphi(u)$, $\varphi(u)$ is then the orientation distribution function (ODF), note that u will always means a vector on the unit sphere S^2 here and below. The normalization of ODF requires

$$\int_{u\in S^2} \varphi(u)\,\mathrm{d}\,u = 1. \tag{2–17}$$

In this case, the revised partition function is then given by

$$Z_{lc}(T,V,N) = \frac{1}{N!\Lambda^{3N}} \int \prod_i \mathrm{d}\,q_i\,\mathrm{d}\,u_i \varphi(u_i) \prod_{i<j} e^{-\beta u(q_i,u_i;q_j;u_j)}, \tag{2–18}$$

and the free energy is calculated

$$\begin{aligned} \frac{\beta}{N}F_{lc} &= -\frac{1}{N}\ln Z_{lc}(T,V,N) \\ &= \ln(\rho\Lambda^3) - 1 + \int_{u\in S^2} \mathrm{d}\,u\varphi(u)\ln\varphi(u) + \frac{\beta}{N}F_{ex}, \end{aligned} \tag{2–19}$$

The first term comes from the free energy of ideal gas (only kinetic energy involved), the second term is the entropy contributed by orientational tendency. The last term is due to the non zero mutual interaction, in particular, if we take a second-order approximation, it can be written as

$$\frac{\beta}{N}F_{ex} = \frac{\rho}{2}\int \mathrm{d}\,u_1\,\mathrm{d}\,u_2\varphi(u_1)\varphi(u_2)\int \mathrm{d}\,q\left(1 - e^{-\beta u(0,u_1;q,u_2)}\right), \tag{2–20}$$

this is due to the contribution of excluded volume.

To summarize what have been done now, we have already pre-assumed that there exists a ODF, and calculated the free energy accordingly. Now we use the minimal free energy principle, the system should reach equilibrium when the free energy reaches its minimum. So we can use variational method to find out the corresponding $\varphi(u)$ to make F_{lc} reaches its minimum. We will derive how this can be done in Chap. 2. Before that, we will introduce more methods to get a better expression for F_{ex}.

2.4 Parsons-Lee's Approximation

Let v_m be the molecular volume, and let $F^* \equiv \beta F/N$ be the reduced free energy, $\eta = \rho v_m$ be the packing fraction, we can rewrite the second-order approximation,

$$\begin{aligned} F_{ex}^* &= \frac{\eta}{2} \int \mathrm{d}\, u_1\, \mathrm{d}\, u_2 \varphi(u_1)\varphi(u_2) V_{ex}^*(u_1, u_2) \\ V_{ex}^*(u_1, u_2) &= \frac{1}{v_m} \int \mathrm{d}\, q \left[1 - e^{-\beta u(0, u_1; q, u_2)}\right] \end{aligned} \tag{2–21}$$

According to Parsons-Lee's approximation based on the equation of state of hard spheres, the coefficient on the left $\eta/2$ can be replaced by $G(\eta)$,

$$G(\eta) = \frac{4\eta - 3\eta^2}{8(1-\eta)^2}. \tag{2–22}$$

It is easily seen that $G(\eta) \sim \eta/2$ when $\eta \to 0$.

2.5 Straley's Method

Straley's method is a useful way to describe the cholesteric phase of a liquid crystal, in particular, it is assumed in every plane of the space, the molecules are still at nematic phase and surely have a preferred orientation, and along the normal direction of the plane, the preferred orientation is rotating. This is the same as the "first assume a distribution, then minimize by variational method" trick proposed by Onsager. To be more precise, write the preferred orientation as

$$n(r) = \cos(qZ)e_1 + \sin(qZ)e_2, \tag{2–23}$$

in which e_1 and e_2 are the unit vector along x-axis and y-axis. And $q = 2\pi/p$ is the pitch wave vector, which describes how fast the preferred orientation is rotating, p is of course the chiral pitch. In the limit of weak chirality, q is relatively small, so it can be approximated by $n(r) = e_1 + qZe_2$.

The second-order approximation of excess free energy can be then written as

$$F_{ex}^* = \frac{\eta}{2} \int \mathrm{d}\, u_1\, \mathrm{d}\, u_2 M_0^*(u_1, u_2)\varphi(u_1)\varphi(u_2) - K_t^* q + \frac{1}{2} K_2^* q^2 \tag{2–24}$$

in which K_t and K_2 are twist elastic contributions

$$\begin{aligned} K_t^* &= -\frac{\eta}{2} \int \mathrm{d}\, u_1\, \mathrm{d}\, u_2 M_1^*(u_1, u_2)\varphi(u_1)\varphi'(u_2)u_{2y} \\ K_2^* &= -\frac{\eta}{2} \int \mathrm{d}\, u_1\, \mathrm{d}\, u_2 M_2^*(u_1, u_2)\varphi'(u_1)\varphi'(u_2)u_{1y}u_{2y} \end{aligned} \tag{2–25}$$

and M_k involved are spatial integrals, in particular, M_0 coincides with the excluded volume,

$$M_k^*(u_1, u_2) = \frac{1}{v_m} \int \mathrm{d}\, q \left[1 - e^{-\beta u(0, u_1; q, u_2)}\right] q_z^k. \tag{2–26}$$

2.6 Joachim's Expression

From the derivation above we can see that the integral of excluded volume is important in the calculation, a crucial approximation is considering a hard sphere chain, in which spheres are connected tangentially, while the case is already resolved by Joachim in 2012, and he gave a concrete expression of the excluded volume of it. Overall he solved the flexible case, in which some of the spheres can rotate around. In a nutshell, the analytic expression of the excluded volume of a rigid chain is given by

$$V_{ex}^{*}(u) = 11 - \frac{3}{m} + 3.5339(m + \frac{1}{m} - 2)\sin\theta, \cos\theta = u \cdot e_3, \tag{2–27}$$

in which m is the length of the chain.

2.7 Variation Method

Variational method is used to find the minimal value of a function in terms of a function, it originates from *brachistochrone curve* problem raised by Johann Bernoulli. To illustrate the idea and practical method to solve a variational method, we take *brachistochrone curve* problem as an example. Before solving this, we state an important lemma,

Lemma 2.1 If $f \in C^{\infty}[a,b]$, and any $h \in C^{\infty}[a,b]$ satisfying $h(a) = h(b) = 0$, the following holds

$$\int_a^b f(x)h(x)\,\mathrm{d}\,x = 0,$$

then $f(x) = 0, \forall x \in (a,b)$.

The proof is omitted since it is easy for anyone who once learned calculus. The *brachistochrone curve* problem is reduced to finding f which makes the following integral minimal

$$A(f) = \int_{x_1}^{x_2} \sqrt{1 + f'^2}\,\mathrm{d}\,x. \tag{2–28}$$

Suppose f is the minimal functional, then for any perturbation $f + \epsilon g, g(x_1) = y_1, g(x_2) = y_2$, it holds that $A(f) \leq A(f + \epsilon g)$. So $G(\epsilon) = A(f + \epsilon g)$ has a minimum at $\epsilon = 0$ for any given g, we then have

$$\frac{\mathrm{d}}{\mathrm{d}\,\epsilon} G(\epsilon)|_{\epsilon=0} = 0. \tag{2–29}$$

Substituting A into Eqn. 2–29, we have

$$\int_{x_1}^{x_2} \frac{f'g'}{\sqrt{1+f'^2}}\,\mathrm{d}\,x = \int_{x_1}^{x_2} g\frac{\mathrm{d}}{\mathrm{d}\,x}\left[\frac{f'}{\sqrt{1+f'^2}}\right]\mathrm{d}\,x = 0. \tag{2–30}$$

Then by the Lem. 2.7, to find f, it suffices to solve the ordinary differential equation

$$\frac{\mathrm{d}}{\mathrm{d}\,x}\left[\frac{f'}{\sqrt{1+f'^2}}\right] = 0. \tag{2–31}$$

This is in fact the Euler-Lagrange equation applying to $\sqrt{1+f'^2}$, but the method used above applies to more complicated functional expressions.

2.8 Iteration Method

Up to now we have all expressions needed, and can use Minimal free energy principal to find out the corresponding ODF.

In principal, we have to minimize Eqn. 3–10, but approximately we may assume the ODF in a cholesteric phase is the same as that in a nematic phase, since cholesteric is locally nematic. Hence we can drop the last two terms which are contributed by chirality.

So now we are using variational method to minimize the free energy in the pure nematic phase, i.e.

$$F_n^* = \ln \eta - 1 + \int \mathrm{d}\, u \varphi(u) \ln \varphi(u) + G(\eta) V_{int} + \frac{\eta}{2} A_{int} \tag{2–32}$$

Now we need to minimize the above expression with respect to $\int \varphi(u)\,\mathrm{d}\,u = 1$, using the variational method introduced above, take $\varphi_\epsilon = \varphi + \epsilon\phi$ then we require

$$\frac{\partial}{\partial \epsilon}\left[F_n^*(\varphi_\epsilon) + \lambda\left(\int \varphi_\epsilon \,\mathrm{d}\, u - 1\right)\right]|_{\epsilon=0} = 0, \forall \phi \tag{2–33}$$

By calculation, this gives

$$\int \mathrm{d}\, u_1 \phi(u_1)\left(1 + \ln\varphi(u_1) + 2G(\eta)\int \mathrm{d}\, u_2 \varphi(u_2) V^*(u_1, u_2)) + \eta \int \mathrm{d}\, u_2 \varphi(u_2) A^*(u_1, u_2)) + \lambda\right) = 0 \tag{2–34}$$

Hence by Lem. 2.7, we have

$$\begin{aligned} 1 + \lambda + \ln\varphi(u_1) + I^{rep}(u_1) + I^{att}(u_1) &= 0 \\ \varphi(u) &= \frac{1}{e^{\lambda+1}} e^{-I^{rep}(u) - I^{att}(u)} \end{aligned} \tag{2–35}$$

in which $e^{\lambda+1}$ is a normalization constant according to the restriction put on φ, and I^{rep}, I^{att} are defined as follows

$$\begin{aligned} I^{rep}(u) &= 2G(\eta)\int \mathrm{d}\, u_2 \varphi(u_2) V^*(u, u_2), \\ I^{att}(u) &= \eta \int \mathrm{d}\, u_2 \varphi(u_2) A^*(u, u_2)). \end{aligned} \tag{2–36}$$

To solve the integral equation given by Eqn. 2–35, use the standard iteration method. Let any reasonable guess of ODF to be φ_0, in particular, it can be Onsager's parametrized ODF:

$$\varphi_0(u) = \frac{\alpha \cosh(\alpha u \cdot e_3)}{4\pi \sinh \alpha}, \tag{2–37}$$

or more simply take to be $\varphi_0(u) \equiv \frac{1}{4\pi}$. Then the iteration goes with

$$\varphi_{n+1}(u) = \mathrm{Norm}\left(e^{-I_n^{rep}(u) - I_n^{att}(u)}\right) \tag{2–38}$$

in which Norm means normalizing the integral over all u to 1.

And iteration stops when $\|\varphi_{n+1} - \varphi_n\|_2 \le 10^{-4}$. To be more precise, the 2-norm for a function defined on a sphere is

$$\|f\|_2 = \int_{u\in S^2} f(u)^2 \,\mathrm{d}\, u. \tag{2–39}$$

Chapter 3 Application to FCh model

3.1 Flexible Chain with Helical Interactions (FCh)

The molecular model is given in Fig. 3–1,

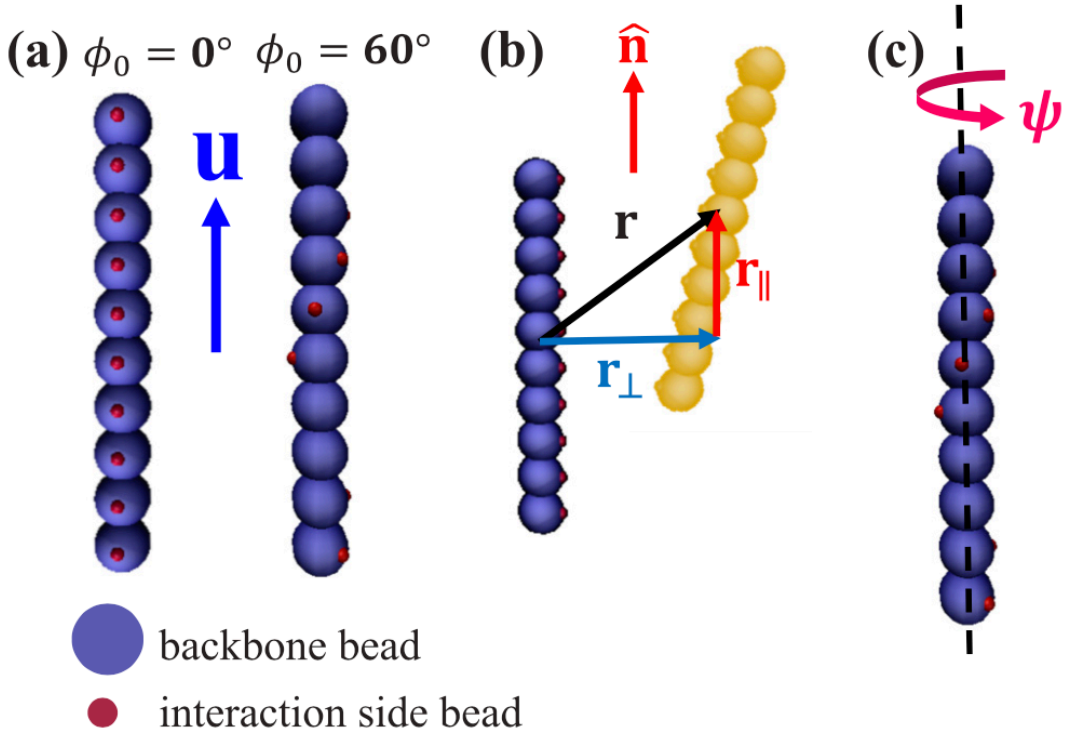

Figure 3–1 Schematic figure of FCh model[12]

There are several defining parameters of a FCh molecule (m, ϕ_0), the former is the length of FCh and the latter is its helix internal angle. In addition, to identify a FCh molecule in the space, it suffices to use (q, u, ϕ), in which q is the position of center of mass, u is the orientation, and ϕ is the internal azimuthal angle.

Denote by σ the length unit, ϵ the energy unit, $\sigma_b = 2^{1/6}\sigma$ and $\sigma_i = 0.1\sigma_b$ are the diameter of the backbone bead and interaction site bead. And there are two kinds of interactions involved, soft repulsion between backbone beads by Weeks-Chandler-Anderson (WCA) potential, short-ranged attractions between interaction beads by shifted Lennard-Jones (sLJ) potential truncated at $r_c = 2.5\sigma$.

$$U_{\mathrm{WCA}}(r) = \begin{cases} 4\epsilon\left[\left(\frac{\sigma_b}{r}\right)^{12} - \left(\frac{\sigma_b}{r}\right)^{6}\right] + \epsilon & r < \sigma_b \\ 0 & r \geq \sigma_b \end{cases} \tag{3–1}$$

$$U_{\mathrm{sLJ}}(r) = \begin{cases} 4\epsilon\left[\left(\frac{\sigma_i}{r}\right)^{12} - \left(\frac{\sigma_i}{r}\right)^{6}\right] - U_{\mathrm{LJ}}\left(r_c\right) & r < 2.5\sigma \\ 0 & r \geq 2.5\sigma \end{cases} \tag{3–2}$$

As for the potential between backbone and interaction beads, it is sLJ potential with parameters are derived by Lorentz-Berthelot mixing rule in the previous simulation work, but here it is ignored, there only b-b interaction and i-i interaction in this theoretical work.

3.2 Existing Simulation Results

Molecular dynamics simulations were performed in the paper and it is found there are three existing phases, isotopic, nematic and cholesteric. To illustrate further, take the example in case of $m = 10, \phi_0 = 30°$, the pressure and phase diagram is shown below.

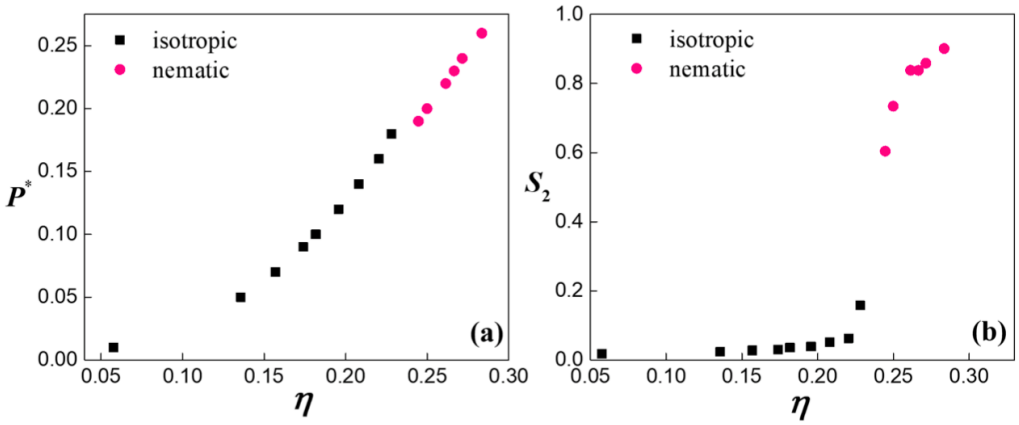

Figure 3–2 Phase Diagram of FCh using MD simulation[12]

Note in the diagram, $P^* = P\sigma^3/\epsilon$. And in this figure we know the transition pressure and transition packing fraction are $P_0^* = 0.1 v_m = 1.332, \eta_0 = 0.24$

3.3 DFT of FCh Model

This part will make use of all the methods introduced before and apply to FCh model. In particular, we will illustrate how to use variational method and iteration to find out ODF which corresponds to the minimal free energy.

Recall that the free energy is unpacked into two parts,

$$F^* = F_{id}^* + F_{ex}^*, \tag{3–3}$$

the first term contains both free energy of ideal gas and the entropy contributed by ODF,

$$F_{id}^* = \ln \eta - 1 + \int \mathrm{d}\, u f(u) \ln f(u), \tag{3–4}$$

in fact the first term is $\ln \rho \Lambda^3$, but this does not matter because it only differs by a constant with $\ln \eta$.

Then due to Straley[13, 14] , the excess free energy is written in the form

$$F_{ex}^* = \frac{\eta}{2}\int \mathrm{d}\,u_1\,\mathrm{d}\,u_2 M_0^*(u_1,u_2)\varphi(u_1)\varphi(u_2) - K_t^* q + \frac{1}{2}K_2^* q^2 \tag{3–5}$$

$$K_t^* = -\frac{\eta}{2}\int \mathrm{d}\,u_1\,\mathrm{d}\,u_2 M_1^*(u_1,u_2)\varphi(u_1)\varphi'(u_2)u_{2y} \tag{3–6}$$

$$K_2^* = -\frac{\eta}{2}\int \mathrm{d}\,u_1\,\mathrm{d}\,u_2 M_2^*(u_1,u_2)\varphi'(u_1)\varphi'(u_2)u_{1y}u_{2y} \tag{3–7}$$

and in which M_k has been defined above.

In addition, the first term of F_{ex}^* can be further divided into repulsion part and attractive part, the repulsion part can then be approximated by Parsons-Lee's method,

$$\frac{\eta}{2}\int \mathrm{d}\,u_1\,\mathrm{d}\,u_2 M_0^*(u_1,u_2)\varphi(u_1)\varphi(u_2) = G(\eta)V_{int} + \frac{\eta}{2}A_{int}. \tag{3–8}$$

in which V_{int} and A_{int} is the abbreviation for two integrals, they will be used further in the calculation of other physical properties,

$$\begin{aligned} V^*(u_1,u_2) &= \frac{1}{v_m}\int \mathrm{d}\,q\left[1-e^{-\beta U_{rep}(0,u_1;q,u_2)}\right], \\ V_{int} &= \int \mathrm{d}\,u_1\,\mathrm{d}\,u_2 V^*(u_1,u_2)\varphi(u_1)\varphi(u_2), \\ A^*(u_1,u_2) &= \frac{1}{v_m}\int \mathrm{d}\,q\left[1-e^{-\beta U_{att}(0,u_1;q,u_2)}\right], \\ A_{int} &= \int \mathrm{d}\,u_1\,\mathrm{d}\,u_2 A^*(u_1,u_2)\varphi(u_1)\varphi(u_2). \end{aligned} \tag{3–9}$$

According to Sec. 2.6, the expression for V^* can be approximated directly by Eqn. 2–27, since the repulsion interaction in FCh model is nearly hard.

Up to now all the required quantities are presented. In the next section we write down explicitly all the important physical properties.

3.4 Properties

All the properties calculated in this part should be calculated after computing ODF using iteration method, but for logical coherence, we derive them first.

Remark: keep in mind that $F^* \equiv \beta F/N$.

3.4.1 Reduced free energy

The general expression of reduced free energy can be collected into one expression

$$F^* = \ln\eta - 1 + \int \mathrm{d}\,u\varphi(u)\ln\varphi(u) + \frac{4\eta-3\eta^2}{8(1-\eta)^2}V_{int} + \frac{\eta}{2}A_{int} - K_t^* q + \frac{1}{2}K_2^* q^2. \tag{3–10}$$

To be more precise, the expression above is the free energy of cholesteric phase, as for the free energy of nematic phase, the last two terms are dropped

$$F_n^* = \ln\eta - 1 + \int \mathrm{d}\,u\varphi(u)\ln\varphi(u) + \frac{4\eta-3\eta^2}{8(1-\eta)^2}V_{int} + \frac{\eta}{2}A_{int}. \tag{3–11}$$

And as for the free energy of isotropic phase, it suffices to let $\varphi(u) \equiv \frac{1}{4\pi}$ and substitute into Eqn. 3–11.

3.4.2 Reduced Pressure

The reduced pressure $P^* = \beta v_m P = -\beta v_m \frac{\partial F}{\partial V} = \eta^2 \frac{\partial F^*}{\partial \eta}$

$$P^* = \eta + \frac{\eta^2(2-\eta)}{4(1-\eta)^3} V_{int} + \frac{1}{2}\eta^2 A_{int} - \frac{1}{2}\eta K_t^* q \tag{3–12}$$

3.4.3 Chemical Potential

The reduced chemical potential $\mu^* = \beta\mu = \beta \frac{\partial F}{\partial N} = \eta \frac{\partial F^*}{\partial \eta} + F^*$

$$\mu^* = \ln \eta + \int \mathrm{d}\, u \varphi(u) \ln \varphi(u) + \frac{\eta(3\eta^2 - 9\eta + 8)}{8(1-\eta)^3} V_{int} + \eta A_{int} - K_t^* q. \tag{3–13}$$

3.4.4 Order Parameter

The order parameter is standard from Onsager's theory

$$S_2 = \int \mathrm{d}\, u \varphi(u) \left[\frac{1}{2}(3\cos^2\theta - 1) \right], \tag{3–14}$$

in which θ is the angle between u and e_3, precisely given by $\cos\theta = u_z = u \cdot e_3$.

3.5 Code Calibration: Hard Spherocylinders (HSC) Model

To verify the correctness of the computation program, we used the data from Jackson's work[3] in 1996. In the paper the author re-examined the phase diagram of hard spherocylinders by Monte-Carlo simulation in a canonical ensemble. The schematic of hard spherocylinders is given below. We used our theoretical method to calculate the phase diagram of HSC, and the result is in well accordance with Jackson's simulation results.

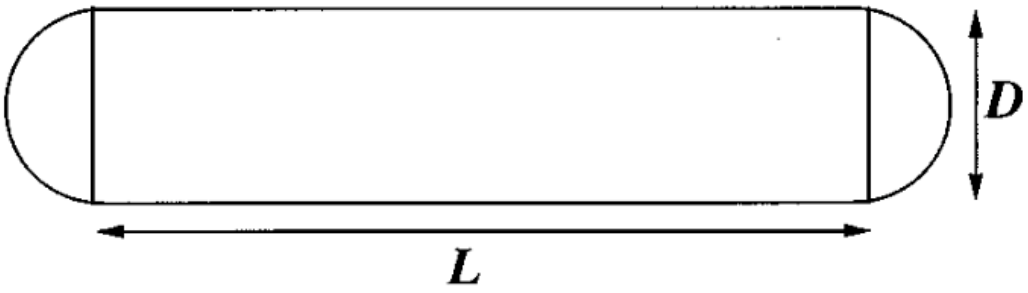

Figure 3–3 Schematic of Hard Spherocylinders[3]

Jackson et al. calculated HSC with four different ratio of length and diameter $\kappa = L/D = 3, 3.2, 4, 5$, and the nematic-isotropic transition point is compared in the next table.

Table 3–1 Comparison of transition point

	$\kappa = 3$	$\kappa = 3.2$	$\kappa = 4$	$\kappa = 5$
η_{MC}	0.577	0.513	0.472	0.408
η_{DFT}	0.530	0.515	0.460	0.405

It can be seen from Tab. 3–1 that the result given by DFT method is in accordance with the result given by Monte Carlo method in a canonical ensemble. The more detailed data of pressure is also in well accordance.

3.6 Program Development

To calculate all the properties and phase diagram mentioned above, a whole program in C++ has been implemented from scratch and been uploaded on Github. The program is transferrable for different kind of liquid crystals as long as the class which defined the molecule structure is added.

Overall, the program contains three main features

1. Monte Carlo computation of ensemble average of quantities in terms of energy.
2. Computation of ODF by iteration method.
3. Calculation of free energy and remaining physical properties.

And this section serve as both a report for what has been done and instructions for those who need to continue the liquid crystal project study. We first recapitulate the expressions we are going to compute, and further in following chapters we illustrate concrete implementation involved.

3.6.1 Monte Carlo Method

According to the theory introduced before, we need to first calculate properties which are irrelevant to ODF, namely, they are A^*, V^*, M_k^* (which are given by Eqn. 3–9, Eqn. 2–26). To see how they are calculated, V^* has been given by Joachim's approximation in Eqn. 2–27. And A^*, M_k^* are computed using Monte Carlo method.

$$\begin{aligned} V^*(u_1,u_2) &= 11 - \frac{3}{m} + 3.5339(m + \frac{1}{m} - 2)\sin\theta, \cos\theta = u_1 \cdot u_2, \\ A^*(u_1,u_2) &= \frac{1}{v_m}\int \mathrm{d}\, q \left[1 - e^{-\beta U_{att}(0,u_1;q,u_2)}\right], \\ M_k^*(u_1,u_2) &= \frac{1}{v_m}\int \mathrm{d}\, q \left[1 - e^{-\beta u(0,u_1;q,u_2)}\right] q_z^k. \end{aligned}$$

Note that in fact to identify a FCh model, it is necessary to designate at least three parameters: (q, u, ϕ), in which q denotes the coordinate of its center of mass, u denotes its orientation, and ϕ denotes the internal azimuthal angle. So the integral in A^*, M_k^* has to be slightly modified and made more precise:

$$\begin{aligned} A^*(u_1,u_2) &= \frac{1}{v_m}\int_V \mathrm{d}\, q \int_0^{2\pi} \mathrm{d}\,\phi_1 \int_0^{2\pi} \mathrm{d}\,\phi_2 \left[1 - e^{-\beta U_{att}(0,u_1,\phi_1;q,u_2,\phi_2)}\right], \\ M_k^*(u_1,u_2) &= \frac{1}{v_m}\int_V \mathrm{d}\, q \int_0^{2\pi} \mathrm{d}\,\phi_1 \int_0^{2\pi} \mathrm{d}\,\phi_2 \left[1 - e^{-\beta u(0,u_1,\phi_1;q,u_2,\phi_2)}\right] q_z^k. \end{aligned} \tag{3–15}$$

In the expression V is taken to be the whole space in which MC process will take place, and let the length scale on one dimension to be two times of a single molecule, i.e. denote $L = 2m\sigma_b$.

Since the two integrals are of the same type, we only illustrate the computation for M_k^*. By using cylindrical coordinates, write $\mathrm{d}\,q = r\,\mathrm{d}\,r\,\mathrm{d}\,z\,\mathrm{d}\,\phi$. Then the expression of M_k^* becomes

$$M_k^*(u_1, u_2) = \frac{2\pi}{v_m} \int_{-L/2}^{L/2} \mathrm{d}\,z \int_{-L/2}^{L/2} \mathrm{d}\,r \int_0^{2\pi} \mathrm{d}\,\phi_1 \int_0^{2\pi} \mathrm{d}\,\phi_2 \left[1 - e^{-\beta u(0,u_1,\phi_1;q,u_2,\phi_2)}\right] z^k r. \tag{3–16}$$

Except for using Monte Carlo method to estimate the preceding integral, we can also use an averaged method by dividing z, r, ϕ_1, ϕ_2 into uniform pieces. In practice, z, r are always taken to be divided into 50 pieces and ϕ_1, ϕ_2 are divided into 10 pieces.

3.6.1.1 Collision Detection

In the estimation of the integral introduced above, there are many pairs of configurations which made $u(0, u_1, \phi_1; q, u_2, \phi_2) = 0$ and hence contributes nothing to the whole integral, since the interaction between FCh molecules are relatively short-ranged. So we can calculate the shortest distance between two molecules and judge if it is within the cutoff distance to optimize the integral compu-

tation. We give the algorithm here without proof, since it is easy with elementary vector analysis.

Algorithm 3–1 Shortest Distance between a Point and a Segment

Data: point $\vec{p}$, start point of the segment $\vec{s}$, end point of the segment $\vec{t}$

Result: shortest distance d between $\vec{p}$ and the segment defined by $\vec{s}, \vec{t}$

$\vec{u} \leftarrow \dfrac{\vec{t} - \vec{s}}{\|\vec{t} - \vec{s}\|_2}$;

$\vec{ps} \leftarrow \vec{p} - \vec{s}$, $\vec{pt} \leftarrow \vec{p} - \vec{t}$;

if $\vec{u} \cdot \vec{ps} < 0$ **then**

  $d \leftarrow \|\vec{ps}\|_2$;

else if $\vec{u} \cdot \vec{pt} > 0$ **then**

  $d \leftarrow \|\vec{pt}\|_2$;

else

  $d \leftarrow \|\vec{u} \times \vec{ps}\|_2$;

Algorithm 3–2 Shortest Distance between Two Segments

Data: length, center and unit orientation vector of the segment $l_i, \vec{r}_i, \vec{u}_i$

Result: shortest distance d between the two segment

$\vec{s} \leftarrow \vec{r}_1 - \vec{r}_2$;

$f \leftarrow$True;

if $1 - (\vec{u}_1 \cdot \vec{u}_2)^2 = 0$ **then**

  $f \leftarrow$False; `// Parallel segments`

else

  $\lambda_1 \leftarrow \dfrac{1}{1 - (\vec{u}_1 \cdot \vec{u}_2)^2} \left(-\vec{s} \cdot \vec{u}_1 + (\vec{s} \cdot \vec{u}_2)(\vec{u}_1 \cdot \vec{u}_2)\right)$;

  $\lambda_2 \leftarrow \dfrac{1}{1 - (\vec{u}_1 \cdot \vec{u}_2)^2} \left(\vec{s} \cdot \vec{u}_2 - (\vec{s} \cdot \vec{u}_1)(\vec{u}_1 \cdot \vec{u}_2)\right)$;

  if $\left(|\lambda_1| > l_1/2\right) \vee \left(|\lambda_2| > l_2/2\right)$ **then**

    $f \leftarrow$False; `// Skew segments`

  else

    $f \leftarrow$True; `// Segments intesects`

if f **then**

  $d \leftarrow \|\vec{s} + \lambda_1 \vec{u}_1 - \lambda_2 \vec{u}_2\|_2$

else

  d is taken to be the minimum of four shortest distance from four endpoints to the other segments using Alg. 3–1.

Using the algorithms introduced above, the efficiency of Monte Carlo estimation of the integral can be largely improved.

3.6.2 DFT calculation

With all the data coming from the Monte Carlo method, using iteration to find out the corresponding ODF with a given packing fraction η can be directly performed, which has been already illustrated in Sec. 2.8. But to clarify here, we must point out the concrete discretization method

of a function on the sphere. we divide every longitude line into 20 parts, and latitude line into 40 part (except at two poles), so this gives $40 \times 19 + 2 = 762$ point on the sphere. Hence the ODF is actually a 762-dimensional vector in computation code. So $\mathrm{d}\phi = \mathrm{d}\theta = \pi/20$And $\mathrm{d}u$ actually becomes $\frac{\pi^2}{400}\sin\phi$, with $u \cdot e_3 = \cos\phi$.

3.7 Iteration Process

The DFT process should give a convergent result of ODF, we put an example here showing this.

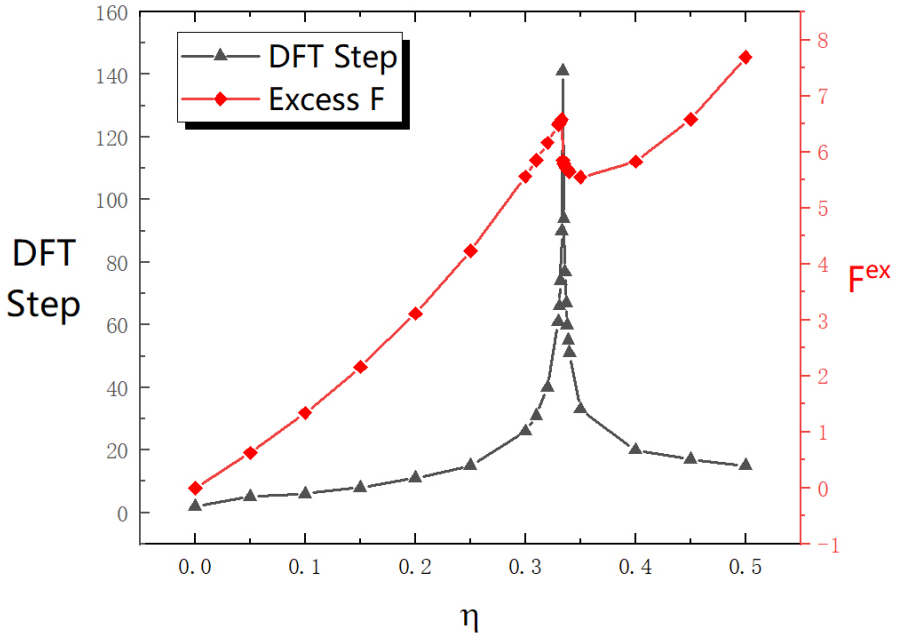

Figure 3–4 Step of DFT process

From this we can see that near the first-order transition point, the iteration step reaches a peak, which means it the state is very non stable near transition and may jump between two different states.

3.8 The Isotropic-Nematic Phase Transition

The isotropic-Nematic phase transition is observed using this theoretical method, and a typical result of physical properties at $m = 10, \phi_0 = 30^\circ$ is given below. A sudden change in the order parameter implies an isotropic-nematic phase transition, and we can also see that the free energy of nematic phase is lower than free energy of isotropic phase.

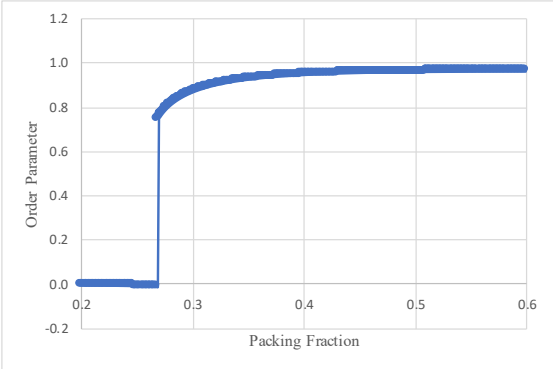

Figure 3–5 Relation between order parameter and packing fraction

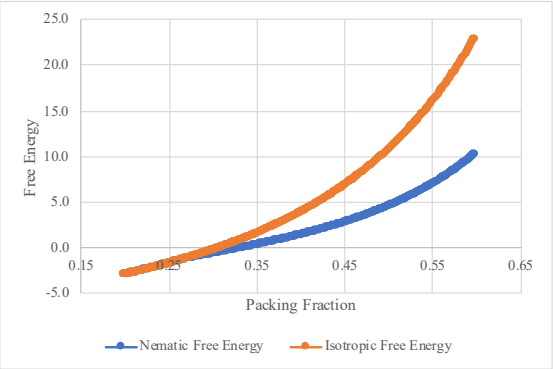

Figure 3–6 Free energy of isotropic and nematic phases

And the sudden change at $\eta = 0.268$ can also be seen in the diagram of pressure and chemical potential, there is a sudden decline as well as the case in free energy. This is the typical characteristic of a first-order transition.

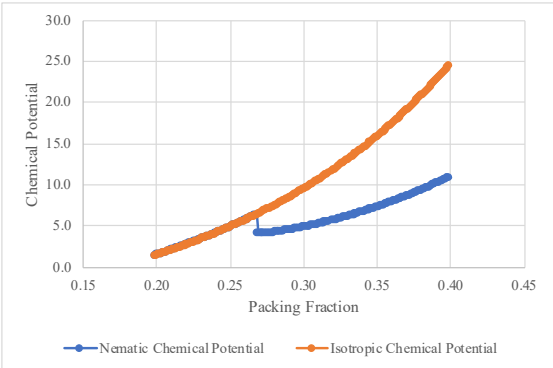

Figure 3–7 Chemical potential of isotropic and nematic phase

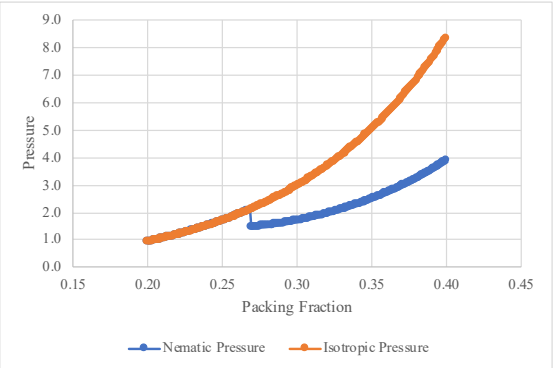

Figure 3–8 Pressure of isotropic and nematic phase

In addition, we compared the transition point at different length and internal azimuthal angle, the following are the data of transition point for FCh model of length $m = 10, 15, 20$ and internal azimuthal angle $\phi_0 = 15^\circ, 30^\circ, 45^\circ, 60^\circ$.

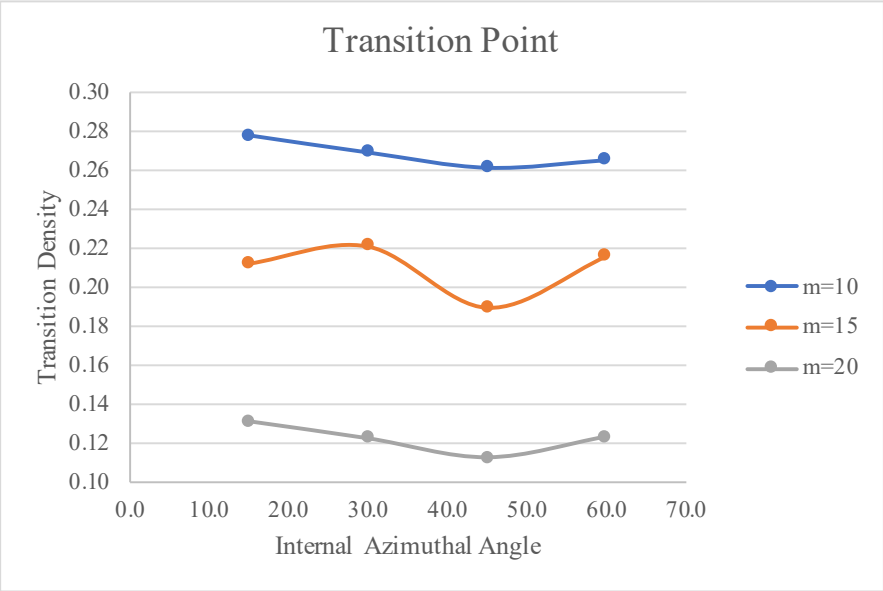

Figure 3–9 Transition point of FCh

It can be seen from the figure that 45° might be a preferred internal azimuthal angle at which two adjacent FCh molecules have the strongest mutual interaction, making it more easily to undergo phase transition. As for a given internal azimuthal angel, the longer the molecule is, the larger its orientational entropy contributes to the free energy, since phase transition is in fact a balance between energy and entropy, the larger contribution from orientational entropy will result in smaller packing fraction.

3.9 The Cholesteric Pitch

The calculation for cholesteric pitch is still not clear since the computation of K_t^* always gives a zero. It is very important here to note when doing integration for M_k^*, we need to make sure that $M_1(u_1,u_2) \neq M_1(u_2,u_1)$, otherwise K_t^* must be zero. This can be seen from the following derivation by writing $\mathrm{d}\,u = \sin\phi\,\mathrm{d}\,\phi\,\mathrm{d}\,\theta$

$$\begin{aligned} K_t^* &= -\frac{\eta}{2}\int \mathrm{d}\,u_1\,\mathrm{d}\,u_2 M_1^*(u_1,u_2)\varphi(u_1)\varphi'(u_2)u_{2y} \\ &= -\frac{\eta}{2}\int_{-\pi/2}^{\pi/2}\mathrm{d}\,\phi_1\varphi(\phi_1)\sin\phi_1\int_{-\pi/2}^{\pi/2}\mathrm{d}\,\phi_2\varphi'(\phi_2)\sin^2\phi_2\int_{-\pi}^{\pi}\mathrm{d}\,\theta_2\sin\theta_2\int_{-\pi}^{\pi}\mathrm{d}\,\theta_1 M_1^*(\phi_1,\theta_1;\phi_2,\theta_2). \end{aligned} \tag{3–17}$$

Suppose $M_1^*(u_1,u_2) = M_1^*(u_2,u_1)$, then $M_1^*(\phi_1,\theta_1;\phi_2,\theta_2) = M_1^*(\phi_2,\theta_2;\phi_1,\theta_1)$, which then implies $T(\theta_2,\phi_1,\phi_2) = \int_{-\pi}^{\pi}\mathrm{d}\,\theta_1 M_1^*(\phi_1,\theta_1;\phi_2,\theta_2)$ is an even function with respect to all three coordinates. In addition, $\varphi(\phi_1)\sin\phi_1$ is odd in ϕ_1, $\varphi'(\phi_2)\sin^2\phi_2$ is odd in ϕ_2 and $\sin\theta_2$ is odd in θ_2. We conclude that

$$K_t^* = -\frac{\eta}{2}\int_{-\pi/2}^{\pi/2}\mathrm{d}\,\phi_1\varphi(\phi_1)\sin\phi_1\int_{-\pi/2}^{\pi/2}\mathrm{d}\,\phi_2\varphi'(\phi_2)\sin^2\phi_2\int_{-\pi}^{\pi}\mathrm{d}\,\theta_2\sin\theta_2 T(\theta_2,\phi_1,\phi_2) = 0 \tag{3–18}$$

So there is something tricky in the Eqn. 3–16, if we write

$$E(u_1,u_2) = \int_0^{2\pi}\mathrm{d}\,\phi_1\int_0^{2\pi}\mathrm{d}\,\phi_2\left[1-e^{-\beta u(0,u_1,\phi_1;q,u_2,\phi_2)}\right], \tag{3–19}$$

Then it is worth thinking how to use a strategy in the Monte Carlo process to guarantee that $E(u_1, u_2) \neq E(u_2, u_1)$.

Up to now the calculation of K_t^* always gives zero, so here we'll present some results on the scaling relation between S and K_2^* near the transition point.

Below is a typical figure of the scaling relation between K_2^* and S for $m = 10, \phi_0 = 30°$,

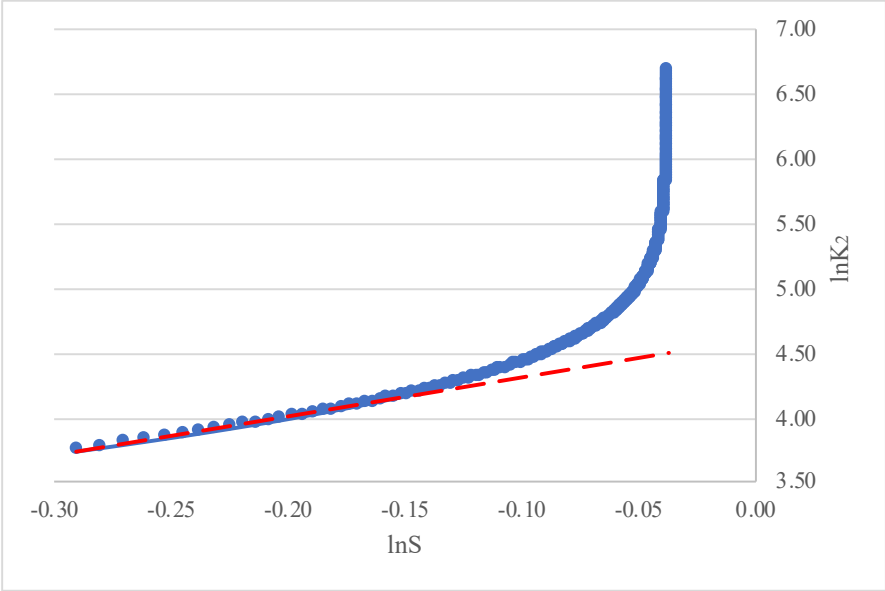

Figure 3–10 Scaling Relation

The slope is 3.02, which implies $K_2^* \sim S^3$ at moderate nematic order.

3.10 Comparison with Simulation Results

Comparing with the simulation results in Sec. 3.2, we can see if our theory gives a very close result with the simulations on the isotropic-nematic transition point.

Table 3–2 Comparison with Simulation

Transition Point	Pressure P_0^*	Packing Fraction η_0
Theory	1.451	0.269
Simulation	1.332	0.240

From Tab. 3–2 we can see that both transition pressure and packing fraction are very close. The transition pressure and packing is a bit larger than that of the simulation. This is due to the assumption that the two-body radial distribution function to be 1. If the correct RDF is calculated, particles that and lean on each other at a short distance and on a preferred angle will contribute more to the free energy calculation, which will lower the transition point. This is the motivation of our future work.

Chapter 4 Summary and Prospect

4.1 Summary

This undergraduate thesis investigated LCh molecule model, a typical kind of liquid crystal with helix interactions. In principle, they are supposed to behave isotropically under under high temperature or very low density, which is the isotropic phase and anisotropically under high density or low temperature where molecules are oriented preferably in a certain direction. And further if they have chiral mutual interactions between each other, they tend to lean on each other with a preferable non zero angle, behaving periodically in the space, which is the cholesteric phase. These phenomena are observed in both experiments and simulations[11]. So a theoretical method is developed in this thesis to give a prediction of the thermodynamic properties of FCh model. The theory is based on Onsager's original theory[1] of phase transition of liquid crystals, and makes use of DFT method to give a depiction of the thermodynamic properties of the phase transition of FCh. In addition, a modular program is developed from scratch for the phase diagram computation of a wide range of liquid crystal molecules including FCh.

4.2 Prospect on Computation of RDF

As is stated in the previous chapter, the lack of accurate RDF accounts that the transition density of theory is slightly larger that that of the theory. We then tried to solve the radial distribution function (RDF) for FCh model, using the Percus-Yevick equation, we write the overall ideas and difficulties. Hope those who are interested in the study of RDF focus on the essential problem raised here.

The Ornstein-Zernike equation is proposed to solve the radial distribution function (RDF), let $h(r) = g(r) - 1$ be the total correlation function, then it can be split into two parts according to Ornstein and Zernike[15],

$$h(|r_1 - r_2|) = c(|r_1 - r_2|) + n \int \mathrm{d}\, r_3 c(|r_1 - r_3|) h(|r_3 - r_3|) \tag{4–1}$$

in which $c(r)$ is the direct correlation. Then the Percus-Yevick approximation gives $c(r) = f(r)y(r)$, $f(r) = e^{-\beta u(r)} - 1$ is the Mayer's function, $y(r) = e^{\beta u(r)} g(r)$ is the background correlation function. Then the Percus-Yevick equation is given by

$$y(|r_1 - r_2|) = 1 + n \int \mathrm{d}\, r_3 f(|r_1 - r_3|) y(|r_1 - r_3|) h(|r_2 - r_3|). \tag{4–2}$$

The equation has an analytic solution for hard spheres according to Wertheim[16]. Lago et al. also have great work[17] on the approximate solution of Percus-Yevick equation of square well spherocylinders. To be more precise, the OZ and PY equation for a rod-like molecule should be modified as follows:

$$\begin{aligned} h(r_1, u_1; r_2, u_2) &= c(r_1, u_1; r_2, u_2) + n \int \mathrm{d}\, r_3 \frac{\mathrm{d}\, u_3}{4\pi} h(r_1, u_1; r_3, u_3) c(r_2, u_2; r_3, u_3) \\ y(r_1, u_1; r_2, u_2) &= 1 + n \int \mathrm{d}\, r_3 \frac{\mathrm{d}\, u_3}{4\pi} f(r_1, u_1; r_3, u_3) y(r_1, u_1; r_3, u_3) h(r_2, u_2; r_3, u_3). \end{aligned} \tag{4–3}$$

And the Percus-Yevick approximation is as same as the preceding one. To decouple the distance parameter and orientation parameter, Lago et al. used an interpolation method to split the background correlation in four main parts, i.e.

$$\begin{aligned} y(r,\alpha,\beta,\theta) =& y_{HT}(r) + \left[y_P(r) - y_{HT}\left(r_{12}\right)\right]\sin\theta \\ &+ \left[y_C(r) - y_P(r)\right]\sin\alpha \\ &+ \left[y_T(r) - y_P(r)\right]\sin\beta. \end{aligned} \tag{4–4}$$

In the equations, α, β, θ are defined in Fig. 4–1. And HT means head-to-tail configuration, P means parallel, C means cross, and T means T-shape. And they can be solved respectively (this is not clear in the original paper), we logically infer to solve them individually, it suffices to solve four integral equation simultaneously (using (i,j) to represent $(r_i,u_i,\phi_i;r_j,u_j,\phi_j)$):

$$\begin{aligned} y_{HT}(12) &= 1 + n\int \mathrm{d}\,r_3 \frac{\mathrm{d}\,u_3}{4\pi} f(13)y(13)h(23), \text{with 1 and 2 are chosen to be head to tail} \\ y_P(12) &= 1 + n\int \mathrm{d}\,r_3 \frac{\mathrm{d}\,u_3}{4\pi} f(13)y(13)h(23), \text{with 1 and 2 are chosen to be parallel} \\ y_C(12) &= 1 + n\int \mathrm{d}\,r_3 \frac{\mathrm{d}\,u_3}{4\pi} f(13)y(13)h(23), \text{with 1 and 2 are chosen to be cross} \\ y_T(12) &= 1 + n\int \mathrm{d}\,r_3 \frac{\mathrm{d}\,u_3}{4\pi} f(13)y(13)h(23), \text{with 1 and 2 are chosen to be T-shape} \end{aligned} \tag{4–5}$$

Together with Eqn. 4–4, the four integral equation can be solved by iteration method in principal, but very hard and time-consuming in practice.

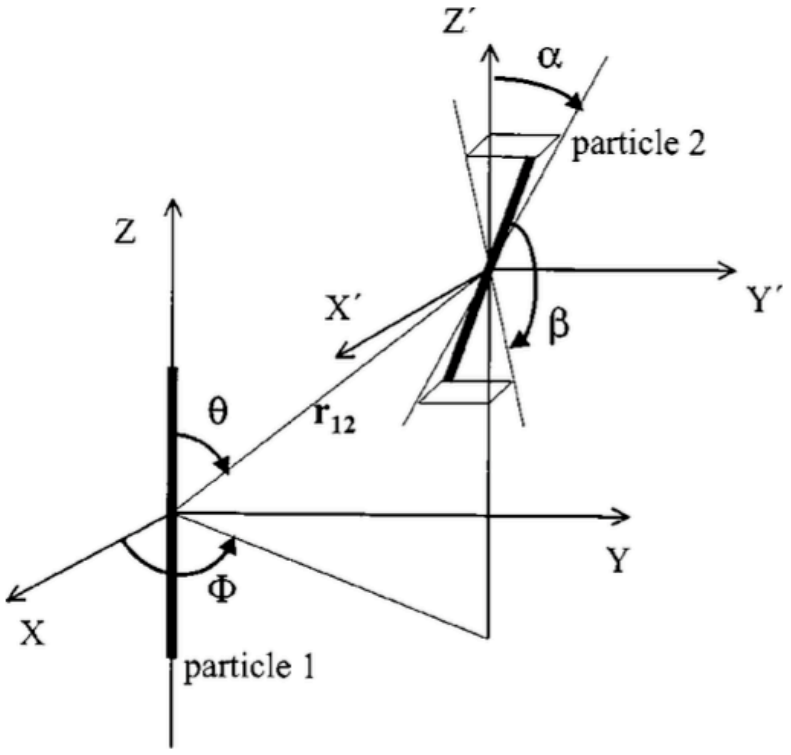

Figure 4–1 Schematic figure of relative coordinates[12]

If we tried to apply to FCh molecule, since it has an additional parameter, the internal azimuthal angle ϕ involved in the integral, namely $\frac{\mathrm{d}\phi}{2\pi}$. The solution of the four integral equations becomes much more impractical.

Bibliography

[1] ONSAGER L. The effects of shape on the interaction of colloidal particles[J]. Annals of the New York Academy of Sciences, 1949, 51(4): 627-659.

[2] WU L, MÜLLER E A, JACKSON G. Understanding and Describing the Liquid-Crystalline States of Polypeptide Solutions: A Coarse-Grained Model of PBLG in DMF[J]. Macromolecules, 2014, 47(4): 1482-1493.

[3] MCGROTHER S C, WILLIAMSON D C, JACKSON G. A re-examination of the phase diagram of hard spherocylinders[J]. The Journal of chemical physics, 1996, 104(17): 6755-6771.

[4] CAPITÁN J A, MARTÍNEZ-RATÓN Y, CUESTA J A. Phase behavior of parallel hard cylinders[J]. Journal of Chemical Physics, 2008, 128(19): 194901.

[5] DOGIC Z, FRADEN S. Ordered phases of filamentous viruses[J]. Current Opinion in Colloid & Interface Science, 2006, 11(1): 47-55.

[6] FURUKAWA R, KUNDRA R, FECHHEIMER M. Formation of liquid crystals from actin filaments[J]. Biochemistry, 1993, 32(46): 12346-12352.

[7] WERBOWYJ R S, GRAY D G. Ordered Phase Formation in Concentrated Hydroxpropylcellulose Solutions[J]. Macromolecules, 1980, 13(1): 69-73.

[8] RAI P K, PARRA-VASQUEZ A N G, CHATTOPADHYAY J, et al. Dispersions of Functionalized Single-Walled Carbon Nanotubes in Strong Acids:Solubility and Rheology[J]. Journal of Nanoscience & Nanotechnology, 2007, 7(10): 3378-3385.

[9] SCHOEN M, HASLAM A J, JACKSON G. Perturbation Theory versus Thermodynamic Integration. Beyond a Mean-Field Treatment of Pair Correlations in a Nematic Model Liquid Crystal.[J]., 2017.

[10] VARGA S, JACKSON G. Study of the pitch of fluids of electrostatically chiral anisotropic molecules: mean-field theory and simulation[J]. Molecular Physics, 2006, 104(22-24): 3681-3691.

[11] WU L, SUN H. Cholesteric ordering predicted using a coarse-grained polymeric model with helical interactions[J]. Soft matter, 2018, 14(3): 344-353.

[12] WU L, SUN H. Manipulation of cholesteric liquid crystal phase behavior and molecular assembly by molecular chirality[J]. Physical Review E, 2019, 100(2): 022703.

[13] Straley, P. J. Frank Elastic Constants of the Hard-Rod Liquid Crystal[J]. Physical Review A, 1973, 8(4): 2181-2183.

[14] STRALEY J P. Theory of piezoelectricity in nematic liquid crystals, and of the cholesteric ordering[J]. Physical Review A, 1976, 14(5): 1835-1841.

[15] ORNSTEIN L S. Accidental deviations of density and opalescence at the critical point of a single substance[J]. Proc. Akad. Sci., 1914, 17: 793.

[16] WERTHEIM M. Exact solution of the Percus-Yevick integral equation for hard spheres[J]. Physical Review Letters, 1963, 10(8): 321.

[17] MARTÍNEZ-HAYA B, CUETOS A, LAGO S. Solution of the Percus-Yevick equation for square well spherocylinders[J]. Physical Review E, 2003, 67(5): 051201.

Acknowledgements

First of all, I am thankful for my parents, who gave me life and raised me up, and most importantly, they are always supporting me to find what I really need. I am also very grateful for my advisor Liang Wu and Huai Sun, they never ceases to encourage me, and helped me a lot in both study and life, Prof. Huai Sun treated me so kind and inspired me a lot to find what I yearn for. And I would like to thank the great teachers I met in Zhiyuan College these four years, Huai Sun and Liang Wu, who led me into this project, Cuipo Jiang, who taught me mathematics and gave me a first taste of modern mathematics, Xiangjun Xing, who gave an impressive lecture on statistical mechanics and enabled me to do hard derivations, Pu Zhang, who treated me so kind and encouragingly and helped a lot when I applied to graduate school. At last, I would thank my friends and classmates, who encouraged and trusted me in the past four years, thanks to Yu Zhou and Yanze Wu, they has guided me a lot when I applied to summer research program, thanks to my roommate Jie Xie, he has helped me a lot on computer technology, and thanks to Yang Zhang who has been my friend for seven years always inspired me when I am down, thanks to Runkang Feng who had helped a lot when I was a freshman in mathematics. I am grateful for been in Zhiyuan College, SJTU for four years, all my experience has made what I am today.